
5-9-2012

Unfolding Prisms as Convex Patches: Counterexamples and Positive Results

Joseph O'Rourke

Smith College, jorourke@smith.edu

Follow this and additional works at: https://scholarworks.smith.edu/csc_facpubs



Part of the [Computer Sciences Commons](#), and the [Geometry and Topology Commons](#)

Recommended Citation

O'Rourke, Joseph, "Unfolding Prisms as Convex Patches: Counterexamples and Positive Results" (2012). *Computer Science: Faculty Publications*. 21.

https://scholarworks.smith.edu/csc_facpubs/21

This Article has been accepted for inclusion in Computer Science: Faculty Publications by an authorized administrator of Smith ScholarWorks. For more information, please contact scholarworks@smith.edu

Unfolding Prismatoids as Convex Patches: Counterexamples and Positive Results

Joseph O’Rourke*

Abstract

We address the unsolved problem of unfolding prismatoids in a new context, viewing a “topless prismatoid” as a *convex patch*—a polyhedral subset of the surface of a convex polyhedron homeomorphic to a disk. We show that several natural strategies for unfolding a prismatoid can fail, but obtain a positive result for “petal unfolding” topless prismatoids. We also show that the natural extension to a convex patch consisting of a face of a polyhedron and all its incident faces, does not always have a nonoverlapping petal unfolding. However, we obtain a positive result by excluding the problematical patches. This then leads a positive result for restricted prismatoids. Finally, we suggest studying the unfolding of convex patches in general, and offer some possible lines of investigation.

1 Introduction

A *prismatoid* is the convex hull of two convex polygons A (above) and B (base) in parallel planes. Despite its simple structure, it remains unknown whether or not every prismatoid has a nonoverlapping edge unfolding, a narrow special case of what has become known as Dürer’s Problem: whether every convex polyhedron has a nonoverlapping edge unfolding [DO07, Prob. 21,1, p. 300]. (All polyhedra considered here are convex polyhedra, and we will henceforth drop the modifier “convex,” and consistently use the symbol \mathcal{P} ; we will also use *unfolding* to mean “nonoverlapping edge unfolding.”) Motivated by the apparent difficulty of placing the top in an unfolding, we explore unfolding *topless prismatoids*, those with the top A removed. We show that several natural approaches fail, but that a somewhat complex algorithm does succeed in unfolding any topless prismatoid.

This success suggests studying the unfolding of a *convex patch* more generally: a connected subset of faces of a polyhedron \mathcal{P} , homeomorphic to a disk. A natural convex patch is an extension of a class studied by Pinciu [Pin07]. He proved that the patch that consists

of one face B of \mathcal{P} and every face that shares an edge with B , has a “petal unfolding” (defined below). This *edge-neighborhood* of a face is itself a natural generalization of “domes,” earlier proven to have a petal unfolding [DO07, p. 323ff]. The generalization we explore is the *vertex-neighborhood* of a face: B together with every face that shares at least a vertex with B . We show that not every vertex-neighborhood patch has a petal unfolding. Note that every topless prismatoid is a vertex-neighborhood of its base. This negative result suggests a restriction that permits unfolding: if \mathcal{P} is nonobtuse triangulated, then the vertex-neighborhood of any face does have a petal unfolding. This in turn leads to a proof that triangular prismatoids (top included), composed of nonobtuse triangles, have an unfolding.

Finally, we make a few observations and conjectures about unfolding arbitrary convex patches.

1.1 Band and Petal Unfoldings

There are two natural unfoldings of a prismatoid. A *band unfolding* cuts one lateral edge and unfolds all lateral faces as a unit, called a *band*, leaving A and B attached each by one uncut edge to opposite sides of the band (see, e.g., [ADL⁺07]). Aloupis showed that the lateral edge can be chosen so that band alone unfolds [Alo05], but I showed that, nevertheless, there are prismatoids such that every band unfolding overlaps [O’R07]. The example will be repeated here, as it plays a role in Sec. 4.

The prismatoid with no band unfolding is shown in Fig. 1. The possible band unfoldings are shown in the Appendix, Figs. 16 and 17. Note that this example also establishes that not every topless prismatoid has a band unfolding, simply by interchanging the roles of A and B .

The second natural unfolding is a *petal unfolding*, called a “volcano unfolding” in [DO07, p. 321]. Because Fig. 1 without its base is a edge-neighborhood patch, it can be petal-unfolded by Pinciu’s result [Pin07] as noted above: simply cut each lateral edge $a_i b_i$.

Let \mathcal{P} be a prismatoid, and assume all lateral faces are triangles, the generic and seemingly most difficult case. Let $A = (a_1, a_2, \dots)$ and $B = (b_1, b_2, \dots)$. Call a lateral face that shares an edge with B a *base* or B -triangle, and a lateral face that shares an edge with A a *top* or

*Department of Computer Science, Smith College, Northampton, MA 01063, USA. orourke@cs.smith.edu. This paper was prepared for but never submitted to *CCCG’12*. It still retains that conference’s formatting conventions.

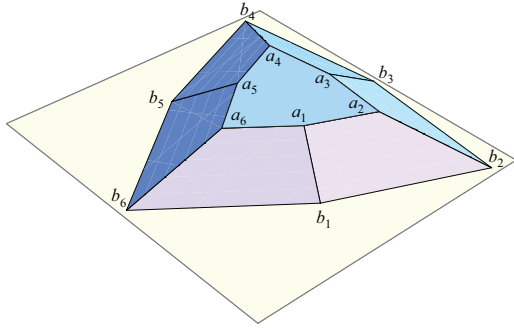


Figure 1: The banded hexagon. The curvatures at the three side vertices $\{a_2, a_4, a_6\}$ is 2° , and that at the apex vertices $\{a_1, a_3, a_5\}$ is 7.5° .

A-triangle. A petal unfolding cuts no edge of *B*, and unfolds every base triangle by rotating it around its *B*-edge into the base plane. The collection of *A*-triangles incident to the same b_i vertex—the *A*-fan AF_i —must be partitioned into two groups, one of which rotates clockwise (cw) to join with the unfolded base triangle to its left, and the other group rotating counterclockwise (ccw) to join with the unfolded base triangle to its right. Either group could be empty. Finally, the top *A* is attached to one *A*-triangle. So a petal unfolding has choices for how to arrange the *A*-triangles, and which *A*-triangle connects to the top. See Fig. 15 in the Appendix for an example.

As of this writing, it remains possible that every prisma-toid has a petal unfolding: I have not been able to find a counterexample. For a hint of why placing the top in a petal unfolding seems problematical, see Fig. 18 in the Appendix. The next section presents the main result: every topless prisma-toid has a petal unfolding.

2 Topless Prisma-toid Petal Unfolding

An example of a petal unfolding of a topless prisma-toid is shown in Fig. 2. Even topless prisma-toids

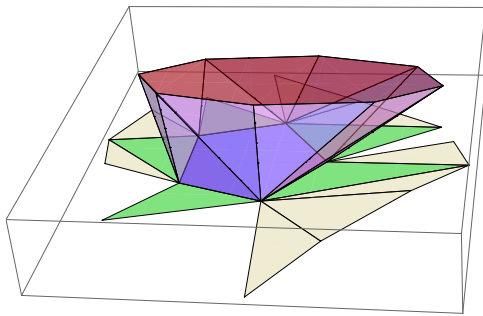


Figure 2: Unfolding of a topless prisma-toid

present challenges. For example, consider the special case when there is only one *A*-triangle between every

two *B*-triangles. Then the only choice for placement of the *A*-triangles is whether to turn each ccw or cw. It is natural to hope that rotating all *A*-triangles consistently ccw or cw suffices to avoid overlap, but this can fail, as in Fig. 18, and even for triangular prisma-toids, Fig. 19 in the Appendix. A more nuanced approach would turn each *A*-triangle so that its (at most one) obtuse angle is not joined to a *B*-triangle (resolving Fig. 19), but this can fail also, a claim I will not substantiate.

The proof follows this outline:

1. An “altitudes partition” of the plane exterior to the *base unfolding* (*B* plus all *B*-triangles) is defined and proved to be a partition.
2. It is shown that both \mathcal{P} and this partition vary in a natural manner with respect to the separation z between the *A*- and *B*-planes.
3. An algorithm is detailed for petal unfolding the *A*-triangles for the “flat prisma-toid” $\mathcal{P}(0)$, the limit of $\mathcal{P}(z)$ as $z \rightarrow 0$, such that these *A*-triangles fit inside the regions of the altitude partition.
4. It is proved that nesting within the partition regions remains true for all z .

2.1 Altitude Partition

We use a_i and b_j to represent the vertices of \mathcal{P} , and primes to indicate unfolded images on the base plane.

Let $B_i = \triangle b_i b_{i+1} a'_i$ be the i -th base triangle. Say that $BU = B \cup (\bigcup_i B_i)$ is the *base unfolding*, the unfolding of all the *B*-triangles arrayed around *B* in the plane, without any *A*-triangles. The altitude partition partitions the plane exterior to the base unfolding.

Let r_i be the *altitude ray* from a'_j along the altitude of B_i . Finally, define R_i to be the region of the plane incident to b_i , including the edges of the B_{i-1} and B_i triangles incident to b_i , and bounded by r_{i-1} and r_i . See Fig. 3.

Lemma 1 *No pair of altitude rays cross in the base plane, and so they define a partition of that plane exterior to the base unfolding BU.*

Proof. See Sec. 5.1 in the Appendix. □

Our goal is to show that the *A*-fan AF_i incident to b_i can be partitioned into two groups, one rotated cw, one ccw, so that both fit inside R_i . (Note that this nesting is violated in Fig. 19 in the Appendix.)

2.2 Behavior of $\mathcal{P}(z)$

We will use “(z)” to indicate that a quantity varies with respect to the height z separating the *A*- and *B*-planes.

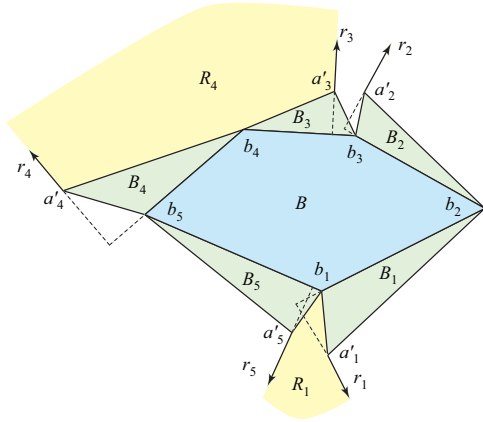


Figure 3: Partition exterior to the base unfolding by altitude rays r_i . In this example both A and B are pentagons; in general there would not be synchronization between the b_i and a_i indices. The A -triangles are not shown.

Lemma 2 Let $\mathcal{P}(z)$ be a prismatoid with height z . Then the combinatorial structure of $\mathcal{P}(z)$ is independent of z , i.e., raising or lowering A above B retains the convex hull structure.

Proof. See Sec. 5.1 in the Appendix. \square

We will call $\mathcal{P}(0) = \lim_{z \rightarrow 0} \mathcal{P}(z)$ a *flat prismatoid*. Each lateral face of $\mathcal{P}(0)$ is either an *up-face* or a *down-face*, and the faces of $\mathcal{P}(z)$ retain this classification in that their outward normals either have a positive or a negative vertical component.

Lemma 3 Let $\mathcal{P}(z)$ be a prismatoid with height z , and $BU(z)$ its base unfolding. Then the apex $a'_j(z)$ of each $B'_i(z)$ triangle $\triangle b_i b_{i+1} a'_j(z)$ in $BU(z)$ lies on the fixed line containing the altitude of $B'_i(z)$.

Proof. See Sec. 5.3 in the Appendix. \square

Thus the vertices $a'_j(z)$ of the base unfolding “ride out” along the altitude rays r_i as z increases (see ahead to Fig. 6 for an illustration). Therefore the combinatorial structure of the altitude partition is fixed, and R_i only changes geometrically by the lengthening of the edges $b_i a'_j$ and $b_{i+1} a'_j$ and the change in the angle gap $\kappa_{b_i}(z)$ at b_i .

2.3 Structure of A -fans

Henceforth we concentrate on one A -fan, which we always take to be incident to b_2 , and so between $B_1 = \triangle b_1 b_2 a_1$ and $B_2 = \triangle b_2 b_3 a_k$. The a -chain is the chain of vertices a_1, \dots, a_k . Note that the plane containing B_1 supports A at a_1 , and the plane containing B_2 supports A at a_k . Let $\beta = \beta_2$ be the base angle at b_2 : $\beta = \angle b_1 b_2 b_3$. We state here a few facts true of every A -fan.

1. An a -chain spans at most “half” of A , i.e., a portion between parallel supporting lines (because $\beta > 0$).
2. If an A -fan is unfolded as a unit to the base plane, the a -chain consists of a convex portion followed by a reflex followed by a convex portion, where any of these portions may be empty. In other words, excluding the first and last vertices, the interior vertices of the chain have convex angles, then reflex, then convex.
3. Correspondingly, an A -fan consists of down-faces followed by up-faces followed by down-faces, where again any (or all) of these three portions could be empty.
4. All four possible combinations of up/down are possible for the B_1 and B_2 triangles.

The second fact above is not so easy to see; its proof is hinted at in Sec. 5.6 in the Appendix. The intuition is that there is a limited amount of variation possible in an a -chain. It is the third fact that we will use essentially; it will become clear shortly.

2.4 Flat Prismatoid Case Analysis

How the A -fan is proved to sit inside its altitude region R for $\mathcal{P}(0)$ depends primarily on where b_2 sits with respect to A , and secondarily on the three B -vertices (b_1, b_2, b_3). Fig. 4 illustrates one of the easiest cases, when b_2 is in C , the convex region bounded by the a -chain and extensions of its extreme edges. Then all the A -faces are down-faces, the a -chain is convex, one of the two B -faces is a down-face (B_2 in the illustration), and we simply leave the A -fan attached to that B down-face.

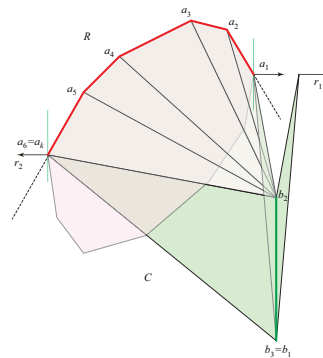


Figure 4: Case 1b. Here we have illustrated $b_1 = b_3$ to allow for the maximum a -chain extent.

A second case occurs when b_2 is on the reflex side of A . An instance when both B -triangles are down-faces is illustrated in Fig. 5. Now the A -fan consists of down-faces and up-faces, the up-faces incident to the reflex

side of the a -chain. These up-faces must be flipped in the unfolding, reflected across one of the two tangents from b_2 to A . A key point is that not always will both flips be “safe” in the sense that they stay inside the altitude region. An unsafe flip is illustrated in Fig. 22 in the Appendix. Fortunately, one of the two flips is

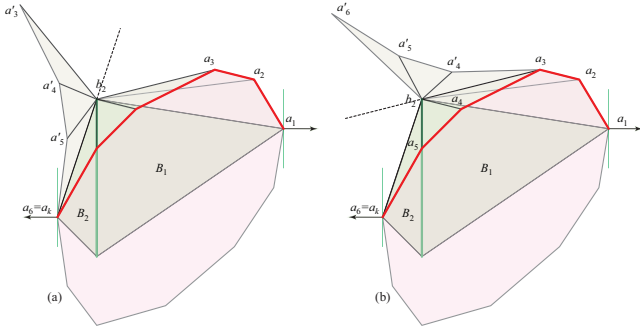


Figure 5: Case 2a. The A -triangles between the tangents b_2 to a_3 and b_2 to a_6 are up-faces. (a) shows the up-faces flipped over the left tangent b_2a_6 , and (b) when flipped over the right tangent b_2a_3 .

always safe:

Lemma 4 *Let b_2 have tangents touching a_s and a_t of A . Then either reflecting the enclosed up-faces across the left tangent, or across the right tangent, is “safe” in the sense that no points of a flipped triangle falls outside the rays r_1 or r_k .*

Proof. See Sec. 5.4 in the Appendix. □

The remaining cases are minor variations on those illustrated, and will not be further detailed. See Fig. 24 in the Appendix.

2.5 Nesting in $\mathcal{P}(z)$ regions

The most difficult part of the proof is showing that the nesting established above for $\mathcal{P}(0)$ holds for $\mathcal{P}(z)$. A key technical lemma is this:

Lemma 5 *Let $\triangle b, a_1(z), a_2(z)$ be an A -triangle, with angles $\alpha_1(z)$ and $\alpha_2(z)$ at $a_1(z)$ and $a_2(z)$ respectively. Then $\alpha_1(z)$ and $\alpha_2(z)$ are monotonic from their $z = 0$ values toward $\pi/2$ as $z \rightarrow \infty$.*

Proof. See Sec. 5.5 in the Appendix. □

I should note that it is not true, as one might hope, that the apex angle at b of that A -triangle, $\angle a_1(z), b, a_2(z)$, shrinks monotonically with increasing z , even though its limit as $z \rightarrow \infty$ is zero. Nor is the angle gap $\kappa_b(z)$ necessarily monotonic. These nonmonotonic angle variations complicate the proof.

Another important observation is that the sorting of ba_i edges by length in $\mathcal{P}(0)$ remains the same for all

$\mathcal{P}(z)$, $z > 0$. More precisely, let $|ba_i| > |ba_j|$ for two lateral edges connecting vertex $b \in B$ to vertices $a_i, a_j \in A$ in $\mathcal{P}(0)$. Then $|ba_i(z)| > |ba_j(z)|$ remains true for all $\mathcal{P}(z)$, $z > 0$ (by reasoning detailed in Lemma 6).

For the nesting proof, I will rely on a high-level description, and one difficult instance. At a high level, each of the convex or reflex sections of the a -chain are enclosed in a triangle, which continues to enclose that portion of the a -chain for any $z > 0$ (by Fact 1, Sec. 5.6). See Fig. 25 in the Appendix for the convex triangle enclosure. The reflex enclosure is determined by the tangents from b_2 to A : $\triangle a_s b_2 a_t$. So then the task is to prove these (at most three) triangles remain within $R(z)$. Fig. 6 shows a case where there is both a convex and a reflex section. Were there an additional convex section, it would remain attached to $B_1(z)$ and would not increase the challenge.

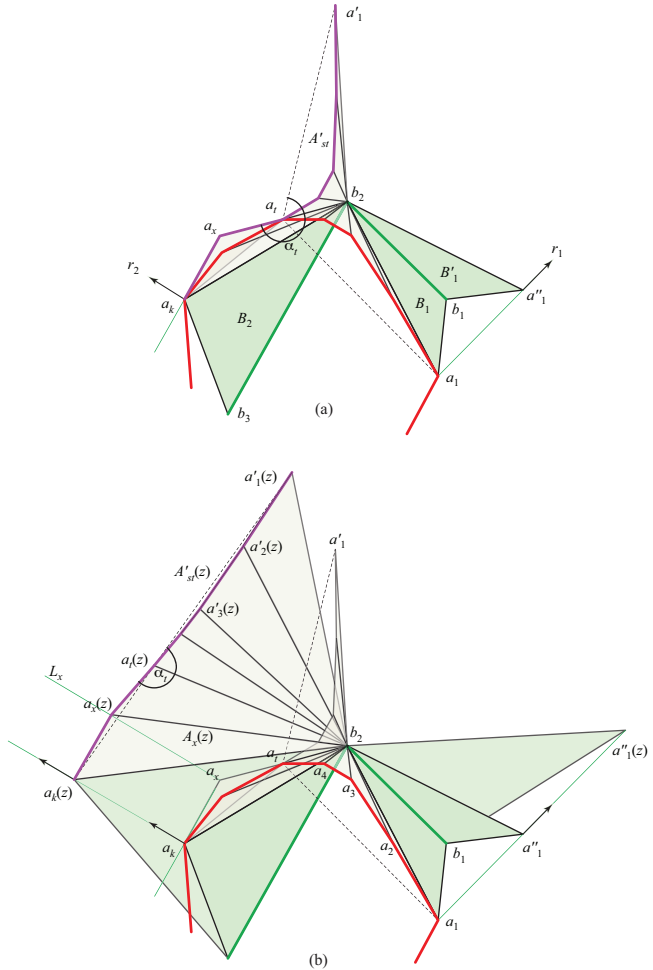


Figure 6: (a) $z = 0$. $\triangle a_t a_x a_k$ encloses the convex section, and $\triangle a_1 b_2 a_t$ encloses the reflex section. (b) $z > 0$. Reflex angle $\alpha_t(z)$ decreases as z increases.

Lemma 6 *If the a -chain consists of a convex and a reflex section, and the safe flip (by Lemma 4) is to a*

side with a down-face (B_2 in the figure), then $AF'(z) \subset R(z)$: the A -fan unfolds within the altitude region for all z .

Proof. See Sec. 5.6 in the Appendix. \square

I have been unsuccessful in unifying the cases in the analysis, despite their similarity. Nevertheless, the conclusion is this theorem:

Theorem 7 *Every triangulated topless prismatoid has a petal unfolding.*

It is natural to hope that further analysis will lead to a safe placement of the top A (which might not fit into any altitude-ray region: see Fig. 18 in the Appendix.

3 Unfolding Vertex-Neighborhoods

Let $N_e(B)$ for a face B of a convex polyhedron \mathcal{P} be B plus the set of all faces that share an edge with B , and $N_v(B)$ be B plus the set of all faces that share a vertex with B . So $N_v(B) \supseteq N_e(B)$. As mentioned previously, Pincu proved that $N_e(B)$ has a petal unfolding. Here we show that $N_v(B)$ does not always have a petal unfolding, even when all faces in the set are triangles.

A portion of the a 9-vertex example \mathcal{P} that establishes this negative result is shown in Fig. 7. The b_1b_3 edge of B lies on the horizontal xy -plane. The vertices $\{b_2, a_1, a_2, c_1, c_2\}$ all lie on a parallel plane at height z , with b_2 directly above the origin: $b_2 = (0, 0, z)$.

All of $N_v(B)$ is shown in Fig. 8. The structure in Fig. 7 is surrounded by more faces designed to minimize curvatures at the vertices b_i of B . Finally, \mathcal{P} is the convex hull of the illustrated vertices, which just adds a quadrilateral “back” face (p_1, c_1, c_2, p_3) (not shown).

The design is such that there is so little rotation possible in the cw and ccw options for the triangles incident to a vertex of B , that overlap is forced: see Figs. 9, 10, and 11. The thin $\triangle b_2a_1a_2$ overlaps in the vicinity of a_1 if rotated ccw, and in the vicinity of a_2 is cw (illustrated). Explicit coordinates for the vertices of \mathcal{P} are given in Sec. 5.7 of the Appendix.

One can identify two features of the polyhedron just described that led to overlap: low curvature vertices (to restrict freedom) and obtuse face angles (at a_1 and a_2) (to create “overhang”). Both seem necessary ingredients. Here I pursue excluding obtuse angles:

Theorem 8 *If \mathcal{P} is nonobtusely triangulated, then for every face B , $N_v(B)$ has a petal unfolding.*

A *nonobtuse triangle* is one whose angles are each $\leq \pi/2$. It is known that any polygon of n vertices has a nonobtuse triangulation by $O(n)$ triangles, which can

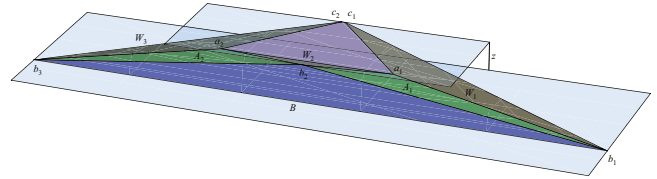


Figure 7: Faces of \mathcal{P} in the immediate vicinity of B .

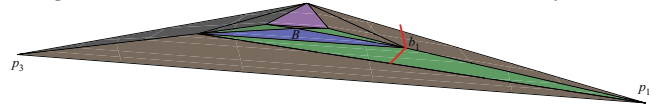


Figure 8: All faces incident to $N_v(B)$, and one more, the purple quadrilateral (a_1, c_1, c_2, a_2) . The red vectors are normal to B and to $\triangle b_1p_1c_1$.

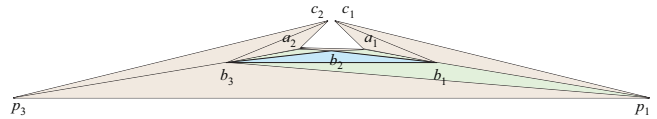


Figure 9: Complete unfolding of all faces incident to B .

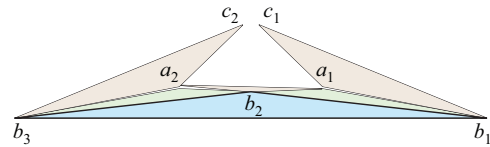


Figure 10: Zoom of Fig. 9.

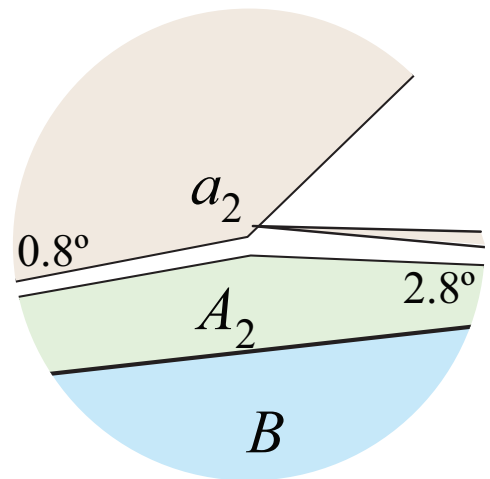


Figure 11: Zoom of Fig. 10 in vicinity of a_2 overlap. The angle gap at b_3 is 0.8° , and the gap at b_2 is 2.8° .

be found in $O(n \log^2 n)$ time [BMR95]. Open Problem 22.6 [DO07, p. 332] asked whether every nonobtusely triangulated convex polyhedron has an edge unfolding. One can view Theorem 8 as a (very small) advance on this problem.

The nonobtuseness of the triangles permits identifying smaller *diamond* regions D_i inside the altitude regions R_i used in Sec. 2, such that D_i necessarily contains the A -fan triangles, regardless of how they are grouped. See Fig. 12(a).

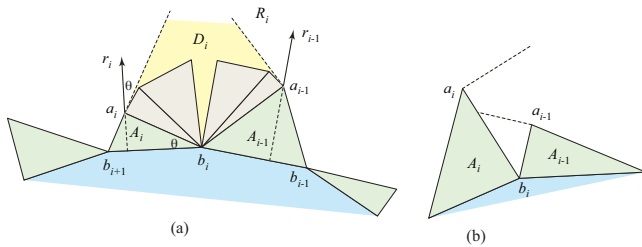


Figure 12: (a) $D_i \subset R_i$. (b) Perpendiculars cannot hit A_i or A_{i-1} .

A little more analysis leads to a petal unfolding of a (very special) class of prisms:

Corollary 9 *Let \mathcal{P} be a triangular prismatoid all of whose faces, except possibly the base B , are nonobtuse triangles, and the base is a (possibly obtuse) triangle. Then every petal unfolding of \mathcal{P} does not overlap.*

Proof. See Sec. 5.8 in Appendix. □

Fig. 13 shows one illustration from the proof, which defines another region $V_i \supset R_i$ which does not overlap the adjacent diamonds D_{i-1} and D_{i+1} , and into which it is safe to unfold the top A .

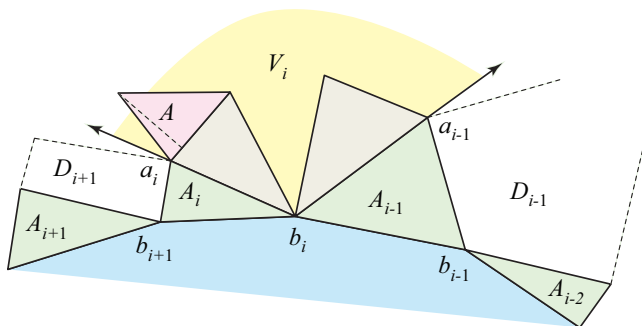


Figure 13: The top A of the prismatoid remains inside V_i .

4 Unfolding Convex Patches

I believe that unfolding convex patches may be a fruitful line of investigation. For example, notice that the

edges cut in a petal unfolding of a topless prismatoid or of vertex-neighborhood of a face, form a disconnected spanning forest rather than a single spanning tree. One might ask: Does every convex patch have an edge unfolding via single spanning cut tree? The answer is NO, already provided by the banded hexagon example in Fig. 1. For such a tree can only touch the boundary at one vertex (otherwise it would lead to more than one piece), and then it is easy to run through the few possible spanning trees and show they all overlap.

The term *zipper unfolding* was introduced in [DDL⁺10] for a nonoverlapping unfolding of a convex polyhedron achieved via Hamiltonian cut path. They studied zipper edge-paths, following edges of the polyhedron, but raised the interesting question of whether or not every convex polyhedron has a zipper path, not constrained to follow edges, that leads to a nonoverlapping unfolding. This is a special case of Open Problem 22.3 in [DO07, p. 321] and still seems difficult to resolve.

Given the focus of this work, it is natural to specialize this question further, to ask if every convex patch has a zipper unfolding, using arbitrary cuts. I believe the answer is negative: a version of the banded hexagon shown in See Fig. 14 has no zipper unfolding. My argument for this is long and seems difficult to formalize, so I leave the claim as a conjecture that, with effort, the proof could be formalized.

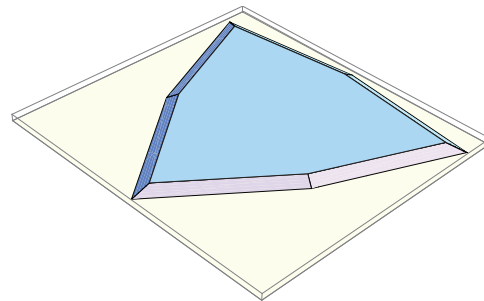


Figure 14: The banded hexagon with a thin band.

References

[ADL⁺07] Greg Aloupis, Erik D. Demaine, Stefan Langermann, Pat Morin, Joseph O’Rourke, Ileana Streinu, and Godfried Toussaint. Edge-unfolding nested polyhedral bands. *Comput. Geom. Theory Appl.*, 39(1):30–42, 2007.

[Alo05] Greg Aloupis. *Reconfigurations of Polygonal Structures*. PhD thesis, McGill Univ., School Comput. Sci., 2005.

[BMR95] Marshall W. Bern, Scott Mitchell, and Jim Ruppert. Linear-size nonobtuse triangulation of polygons. *Discrete Comput. Geom.*, 14:411–428, 1995.

- [DDL⁺10] Erik Demaine, Martin Demaine, Anna Lubiw, Arlo Shallit, and Jonah Shallit. Zipper unfoldings of polyhedral complexes. In *Proc. 22nd Canad. Conf. Comput. Geom.*, pages 219–222, August 2010.
- [DO07] Erik D. Demaine and Joseph O’Rourke. *Geometric Folding Algorithms: Linkages, Origami, Polyhedra*. Cambridge University Press, July 2007. <http://www.gfalop.org>.
- [O’R07] Joseph O’Rourke. Band unfoldings and prisma-toids: A counterexample. Technical Report 087, Smith College, October 2007. arXiv:0710.0811v2 [cs.CG]; <http://arxiv.org/abs/0710.0811>.
- [O’R12] Joseph O’Rourke. Tetrahedron angles sum to π : Bisector plane. MathOverflow: <http://mathoverflow.net/questions/94586/>, April 2012.
- [Pin07] Val Pincu. On the fewest nets problem for convex polyhedra. In *Proc. 19th Canad. Conf. Comput. Geom.*, pages 21–24, 2007.

5 Appendix

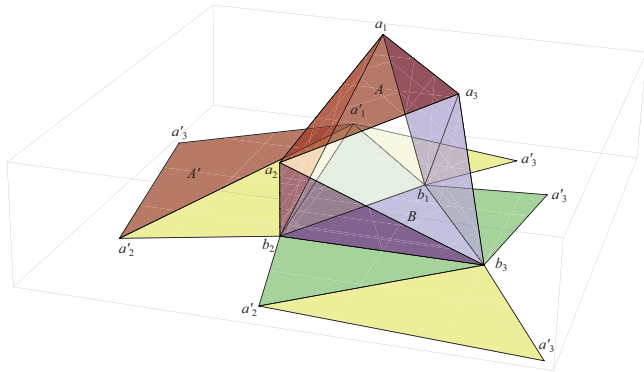


Figure 15: A triangular prismatoid (top and bottom both triangles), and one petal unfolding. The base B -triangles are green; the top A -triangles are yellow.

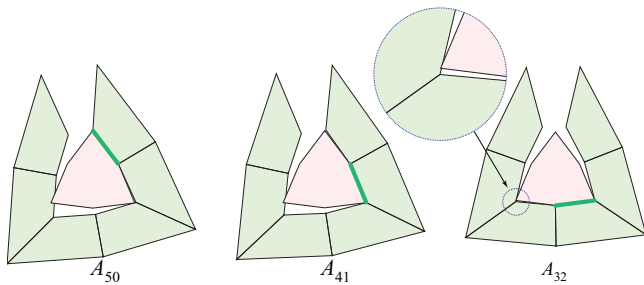


Figure 16: Apex cuts: each leads to overlap. The highlighted edge is not cut.

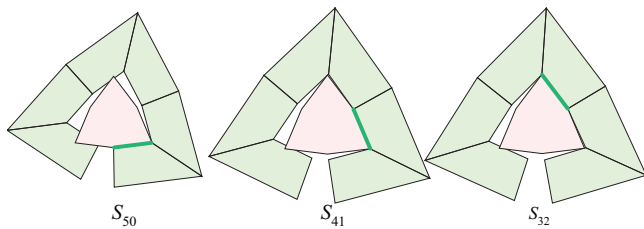


Figure 17: Side cuts: each leads to overlap.

5.1 Proof of Lemma 1

Lemma 1 *No pair of altitude rays cross in the base plane, and so they define a partition of that plane exterior to the base unfolding.*

Proof. Consider three consecutive B vertices of the prismatoid \mathcal{P} , (b_1, b_2, b_3) supporting two base triangles, $B_1 = \triangle b_1 b_2 a_1$ and $B_2 = \triangle b_2 b_3 a_2$. We will show that r_1 and r_2 cannot cross. Let $\beta_1 = \angle b_1 b_2 a_1$ and $\beta_2 = \angle b_3 b_2 a_2$ be the two angles of the base triangles

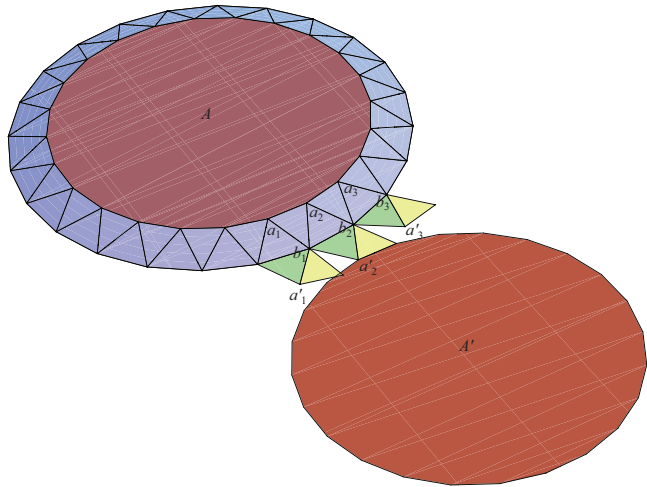


Figure 18: A drum-like prismatoid that results in overlap with consistent cw rotation of the (yellow) A -triangles. Here the point a'_1 overlaps the unfolded top A' . This overlap can be removed easily, by rotating the A -triangle $\triangle a_1 a_2 b_1$ cw rather than ccw.

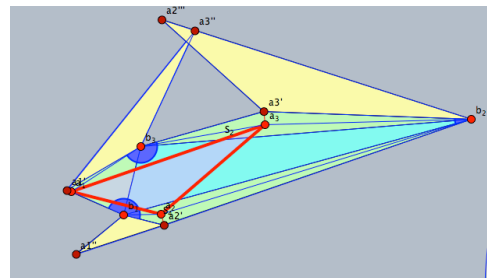


Figure 19: An overhead view of a nearly flat, topless triangular prismatoid. A -triangles $\triangle a_2 a_3 b_2$ and $\triangle a_3 a_1 b_3$ are both rotated ccw, about b_2 and b_3 respectively. [Figure created in Cinderella.]

incident to b_2 . (We use a_2 for the apex of B_2 for simplicity, although there could be intervening A vertices between a_1 and a_2 .) We consider three cases, distinguishing acute and obtuse β_i angles.

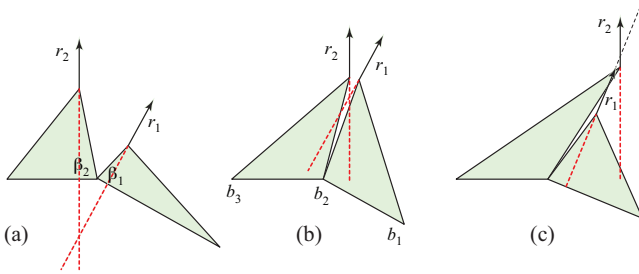


Figure 20: Only in case (c) could ray r_1 cross r_2 .

If both β_1 and β_2 are acute, then the altitudes of B_1 and B_2 lie on the base edges b_1b_2 and b_2b_3 respectively, and the lines containing the rays cross behind the rays, as in Fig. 20(a). Similarly, if both β_1 and β_2 are obtuse, again the ray lines cross behind the rays, this time exterior to B , as in (b) of the figure. Only when one angle is obtuse and the other acute could the rays possibly cross. Without loss of generality, let β_2 be obtuse and β_1 acute, as in (c) of the figure. We now concentrate on this case.

Let H_i be the vertical plane containing the altitude of B'_i . This plane includes both the unfolded a'_i on the B -plane and the vertex a_i on the A -plane, because a'_i is the image of a_i rotated about the base edge b_ib_{i+1} to which the altitude of B_i is perpendicular. See Fig. 21. The B_i triangles of \mathcal{P} cut the A -plane in lines parallel

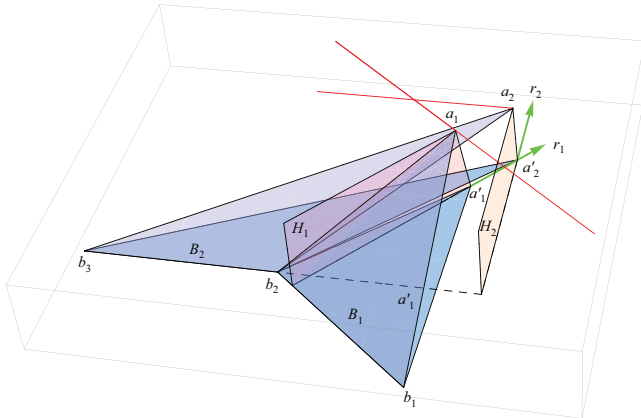


Figure 21: The conditions of this case violate the convexity of \mathcal{P} : a_1 must be right of H_2 so that a_2 is inside the plane determined by B_1 .

to their base edges b_ib_{i+1} , and the top A must fall inside the halfplanes on the A -plane bounded by these lines. Examination of the figure shows that this requires a_1 to lie on the A -plane right of H_2 in the figure. But a'_1 is

necessarily initially left of H_2 if r_1 is to cross r_2 , and the rotation of a'_1 from the B -plane up to the A -plane moves it only further left of H_2 . Thus this last case violates the convexity of \mathcal{P} , and we have established the lemma for adjacent altitude rays r_1, r_2 .

(We have shown in the figure B_1 and B_2 both making an angle less than $\pi/2$ with the base plane, but the argument is not altered if either of those angles exceed $\pi/2$: still the rotation of a_i down to a'_i occurs in the altitude H_i plane.)

Now consider nonadjacent rays, say r_1 and r_i , based on base triangles B_1 and B_i . Extend the edges of those triangles in the B -plane until they meet at point \bar{b} , and form new triangles $\bar{B}_1 = \Delta b_1\bar{b}a_1$ and $\bar{B}_i = \Delta \bar{b}b_{i+1}a_i$ sharing \bar{b} . (Again we use a_i for the apex of B_i without implying there are exactly $i-1$ A -vertices between a_1 and a_i .) Notice these triangles are still apexed at a_1 and a_i respectively, as the planes containing B_1 and B_i support A at these two points. Define $\bar{\mathcal{P}}$ as the convex hull of $\mathcal{P} \cup \bar{b}$. In $\bar{\mathcal{P}}$, the altitudes of the new base triangles \bar{B}_1 and \bar{B}_i are exactly the same as the altitudes of the original B_1 and B_i , because their base edges have been extended while retaining their apexes on A . So the rays r_1 and r_i have not changed in the base plane, and we can reapply the argument for adjacent rays. \square

5.2 Proof of Lemma 2

Lemma 2 *Let $\mathcal{P}(z)$ be a prismatoid with height z . Then the combinatorial structure of $\mathcal{P}(z)$ is independent of z , i.e., raising or lowering A above B retains the convex hull structure.*

Proof. Let $B_1 = \Delta b_1b_2a(z)$ be a B -triangle for some $z > 0$. (The argument is the same for an A -triangle by inverting \mathcal{P} .) Let $L(z)$ be the line in the A -plane parallel to b_1b_2 through $a(z)$, i.e., $L(z)$ is the intersection of the plane containing B_1 with the A -plane. Then $L(z)$ is a line of support for $A(z)$ in the A -plane. As z varies, this line remains parallel to b_1b_2 , and because $A(z)$ merely translates with z (it does not rotate), $L(z)$ remains a line of support to $A(z)$. Thus the plane containing $B_1(z)$ supports $A(z)$, and of course it supports B because b_1b_2 does not move. Therefore, $B_1(z)$ remains a face of $\mathcal{P}(z)$ for all $z > 0$. \square

5.3 Proof of Lemma 3

Lemma 3 *Let $\mathcal{P}(z)$ be a prismatoid with height z , and $BU(z)$ its base unfolding. Then the apex $a'_j(z)$ of each $B'_i(z)$ triangle $\Delta b_ib_{i+1}a'_j(z)$ in $BU(z)$ lies on the fixed line containing the altitude of $B'_i(z)$.*

Proof. Recall that B'_i is produced by rotating B_i about its base edge b_ib_{i+1} . Thus every point on a line perpendicular to b_ib_{i+1} lying within the plane of B_i unfolds to that line rotated to the base plane. Because $a_j(z)$ lies

on such a line containing B_i 's altitude, $a'_j(z)$ is on the line containing the altitude to B'_i . \square

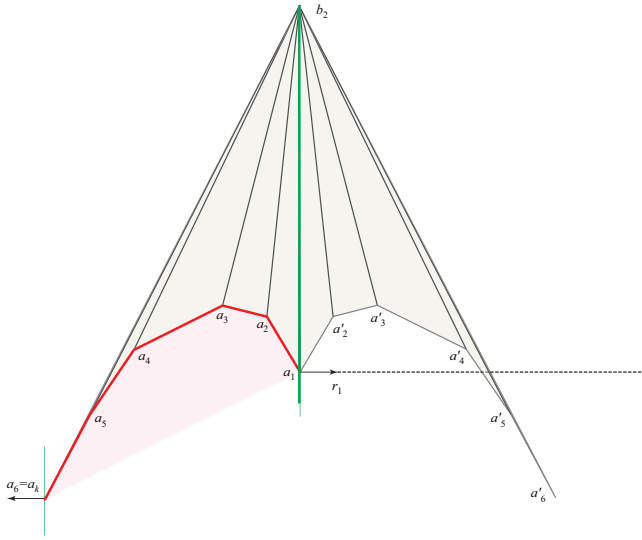


Figure 22: Case 2 gone bad: the chain (a'_4, a'_5, a'_6) leaves R as it crosses r_1 . The overlap in Fig. 19 can also be understood as caused by an unsafe flip.

5.4 Proof of Lemma 4

Lemma 4 *Let b_2 have tangents a_s and a_t to A . Then either reflecting the enclosed up-faces across the left tangent, or across the right tangent, is “safe” in the sense that no points of a flipped triangle falls outside the rays r_1 or r_k .*

Proof. The rays r_1 and r_k are in general below and turned beyond (ccw and cw respectively) the tangency points a_s and a_t , but at their “highest” they are as illustrated in Fig. 23. If reflecting a_s to a'_s is not safe as illustrated, then the perpendicular at a_t must hit $b_2 a_s$. Because it makes an angle β there with $a_t a'_t$, the alternate reflection is safe. \square

5.5 Proof of Lemma 5

Lemma 5 *Let $\triangle b, a_1(z), a_2(z)$ be an A -triangle, with angles $\alpha_1(z)$ and $\alpha_2(z)$ at $a_1(z)$ and $a_2(z)$ respectively. Then $\alpha_1(z)$ and $\alpha_2(z)$ are monotonic from their $z = 0$ values toward $\pi/2$ as $z \rightarrow \infty$.*

Proof. With loss of generality, let $b = (0, 0, 0)$, $a_1(z) = (1, 0, z)$, and $a_2 = (1+x, y, z)$, with $y > 0$. If $x > 0$, then $\alpha_1(z) > \pi/2$ (obtuse), and if $x \leq 0$, then $\alpha_1(z) < \pi/2$ (acute). By symmetry, we need only prove the claim for $\alpha_1(z)$.

The dot-product $(a_1(z) - b) \cdot (a_2(z) - a_1(z))$ determines either $\cos(\alpha_1(z))$ or $\cos(\pi - \alpha_1(z))$, depending on

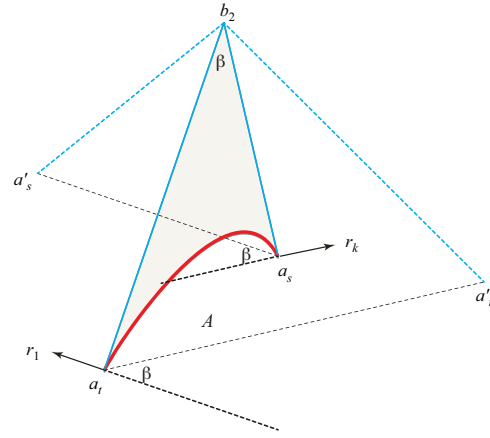


Figure 23: One of the two reflections must remain above the rays r_1 or r_k .

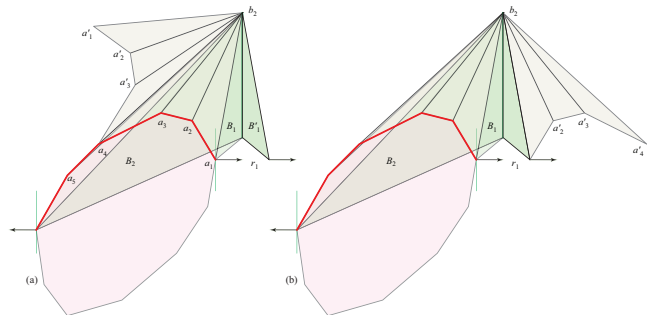


Figure 24: Case 2b. Here B_1 is an up-face. (a) Flip across the left tangent. (b) Rather than flip the up- A -faces across the right tangent, those faces are flipped while attached to B_1 —i.e., we treat B_1 as joined to those up- A -faces.

whether or not $\alpha_1(z)$ is acute or not. Direct computation leads to

$$\cos(\alpha_1) = \frac{x}{\sqrt{x^2 + y^2}\sqrt{1 + z^2}}$$

whose derivative with respect to z is

$$\frac{-xz}{\sqrt{x^2 + y^2}(1 + z^2)^{3/2}}.$$

Because $z > 0$, the sign of the derivative is entirely determined by the sign of x . For α_1 obtuse, $x > 0$, the derivative is negative, which corresponds to decreasing $\alpha_1(z)$, and when $x < 0$ and α_1 is acute, the derivative is positive corresponding to increasing $\alpha_1(z)$. Thus the claim of the lemma is established. \square

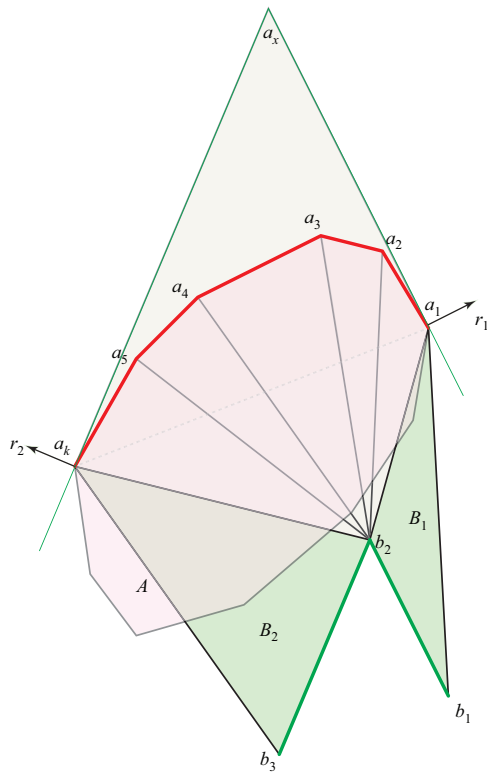


Figure 25: Enclosing a convex chain with a triangle $\triangle a_1 a_x a_k$, where a_x is the intersection of lines of support at a_1 and a_k parallel to $b_1 b_2$ and $b_2 b_3$ respectively.

5.6 Proof of Lemma 6

Here we will need two important facts about the unfolded a -chain:

1. Let α_j be the angle of the chain at a_j , i.e., the sum of the two incident triangle angles, $\angle b_2 a_j a_{j-1} + \angle b_2 a_j a_{j+1}$. If α_j is convex for $z = 0$, it remains convex for all z ; and similarly reflex remains reflex, and a sum of π remains independent of z .

2. $\alpha_j(z)$ is monotonic with respect to z , approaching π as $z \rightarrow \infty$ from above (if initially reflex) or below (if initially convex).

The essence of why Fact 1 holds is in Fig. 26. See [O’R12] for proofs. Fact 2 can be established by

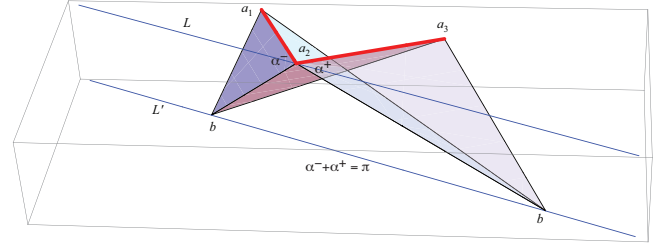


Figure 26: The locus of positions b for which $\alpha^- + \alpha^+ = \pi$

superimposing neighborhoods of a_j for two different z -values $z_1 < z_2$, and noting, for reflex α_j , the z_2 -neighborhood is nested in that for z_1 , and consequently there is a larger curvature $\kappa_{a_j}(z_2) > \kappa_{a_j}(z_1)$.

Lemma 6 *If the a -chain consists of a convex and a reflex section, and the safe flip (by Lemma 4) is to a side with a down-face (B_2 in the figure), then $AF'(z) \subset R(z)$: the A -fan unfolds within the altitude region for all z .*

Proof. Let a_s and a_t be the vertices of the a -chain so that lines containing $b_2 a_s$ and $b_2 a_t$ are supporting tangents to A at a_s and a_t . Thus (a_1, \dots, a_s) represents a convex portion of the a -chain, (a_s, \dots, a_t) the reflex portion, and (a_t, \dots, a_k) a convex portion. We first assume $a_s = a_1$ so we have only a convex and a reflex section, as illustrated in Fig. 6. We also first assume that both B_1 and B_2 are down-faces and so do not require flipping. We analyze this case by mixing the convex and reflex approaches in earlier, easier cases not detailed here (but see Fig. 25).

For the reflex chain, we connect $a_s = a_1$ to a_t to form a triangle $A_{st} = \triangle a_s b_2 a_t$ that encloses the reflex chain. For the convex chain (a_t, \dots, a_k) we intersect the line L_{23} parallel to $b_2 b_3$ through a_k (just as in the all-convex case not detailed), and intersect it with the line containing $b_2 a_t$. Let that intersection point be a_x . Then the triangle $A_x = \triangle b_2 a_x a_k$ encloses the convex chain. Under the assumption that B_1 is a down-face, then A_x encloses all down-faces, and does not need flipping. A_{st} does flip, and let us assume the safe flip is across $b_2 a_t$, flipping a_s to a'_s , with A'_{st} the reflected triangle.

Vertex $a_k(z)$ rides out r_2 . By construction, $a_x(z) a_k(z) \perp r_2$, as a_x was defined by L_{23} parallel to r_2 . Because $|a_x(z) a_k(z)| = |a_x a_k|$, $a_x(z)$ rides out along a line parallel L_x to r_2 , so $A_x(z) \subset R(z)$.

Now the curvature $\kappa(z)$ at b_2 , i.e., the angle gap in the unfolding, varies in a possibly complex way, but it

remains positive at all times, because clearly $\mathcal{P}(z)$ is not flat at b_2 for any z . Thus $b_2a'_1(z)$ is rotated ccw from $b_2a_1(z)$. It remains to show that $b_2a'_1(z)$ cannot cross r_2 .

By Fact 1 above, the convex angle at a_x remains convex at $a_x(z)$, and therefore $a_t(z)$ cannot cross L_x let alone r_2 . Again by Fact 1, the reflex chain (a_1, \dots, a_t) remains a reflex chain with increasing z , and so is contained inside $A'_{st}(z)$. This reflex chain straightens, approaching the segment $a_t(z)a'_1(z)$.

Because that chain is reflex, the only way that A'_{st} can cross r_2 is for the segment $a_t(z)a'_1(z)$ to cross, i.e., for $a'_1(z)$ to cross. Notice this requires a highly reflex angle $\alpha_t(z) = \angle a'_1(z), a_t(z), a_x(z)$, at least $3\pi/2$ in fact, in order to cross over the line L_x . Now we have no control over the initial value of α_t , but we know that the flip was safe, so initially a'_1 is inside r_2 . If α_t is convex, then $\alpha_t(z)$ remains convex and $a'_1(z)$ cannot cross r_2 . So assume α_t is initially reflex (as illustrated in Fig. 6). Then by Fact 2, it decreases monotonically toward π as z increases. Because it decreases, and needs to be at least $3\pi/2$ to cross r_2 , it must have started out at least $3\pi/2$. Now we argue that this is impossible, as the other flip would have been chosen.

As Fig. 27 shows, if $\alpha_t > 3\pi/2$, then the reflection $a_t a'_1$ is already more than $\pi/2$ ccw of $b_2 a_t$, which marks it as an unsafe flip. We would instead have flipped the reflex portion across $b_2 a_1 = a_s$. And indeed the flip in Fig. 6 would not have been chosen because it is potentially unsafe (but does not in this case actually place a'_1 on the wrong side of r_2).

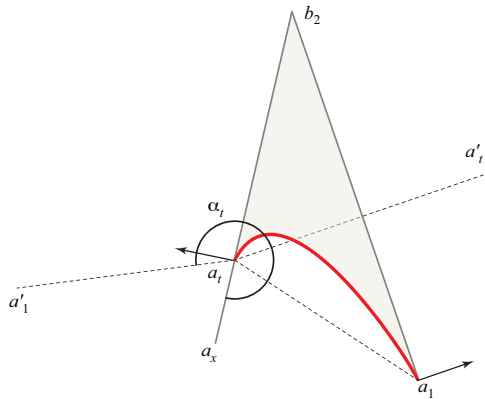


Figure 27: In order for $\alpha_t > 3\pi/2$, $a_t a_1$ must make an angle more than $\pi/2$ with $b_2 a_t$.

□

5.7 Vertex-Neighborhood Counterexample Coordinates

The coordinates of the nine vertices comprising \mathcal{P} in Fig. 7 are shown in the table below, with $\{a_2, b_3, c_2, p_3\}$

each reflections of $\{a_1, b_1, c_1, p_1\}$ with respect to the $x = 0$ plane:

Point	Coordinates
b_2	(0, 0, 0.2)
a_1, a_2	($\pm 0.603496, 0.0399127, 0.2$)
b_1, b_3	($\pm 2, -0.1, 0$)
c_1, c_2	($\pm 0.0124876, 0.501659, 0.2$)
p_1, p_3	($\pm 6.03626, -0.4, -0.6$)

5.8 Proof of Corollary 9

Corollary 7 *Let \mathcal{P} be a triangular prismatoid all of whose faces, except possibly the base B , are nonobtuse triangles, and the base is a (possibly obtuse) triangle. Then every petal unfolding of \mathcal{P} does not overlap.*

Proof. We first let B be an arbitrary convex polygon. We define yet another region $V_i \supset R_i$ incident to b_i , bound by rays from b_i through a_{i-1} and through a_i . See Fig. 13. Note that these rays shoot at or above the adjacent diamonds D_{i-1} and D_{i+1} , and therefore miss A_{i-2} and A_{i+1} .

Now we invoke the assumption that B is a triangle: In that case, those adjacent diamonds contain all the remaining A -triangles, because there are only three b_i vertices: b_1 at which V_1 is incident, and diamonds D_2 and D_3 to either side. (Note there can only be altogether three A -triangles, one for each edge of A .) Now unfold the top A of \mathcal{P} attached to some A -triangle, without loss of generality a A -triangle incident to b_1 . Then because A is nonobtuse, its altitude, and indeed all of A , projects into that edge shared with a A -triangle A_1 . Because the top of the A -triangle is inside D_1 , we can see that $A \subset V_i$, and we have protected A from overlapping any other A -triangle or any A_i . □

It seems quite likely that this corollary still holds with B an arbitrary convex polygon, but, were the same proof idea followed, it would require showing that V_i does not intersect nonadjacent diamonds or more distant A_j triangles.